J Comput Aided Mol Des (2008) 22:563–570
DOI 10.1007/s10822-008-9200-0

Computational prediction of ion permeation characteristics in the glycine receptor modified by photo-sensitive compounds

Mary Hongying Cheng · Rob D. Coalson · Michael Cascio · Maria Kurnikova

Received: 2 November 2007 / Accepted: 18 February 2008 / Published online: 27 March 2008

Abstract We conduct computational analyses of ion permeation characteristics in a model glycine receptor (GlyR) modified by photo-sensitive compounds. In particular, we consider hypothetical attachment to the channel of charge-neutral chemical groups which can be photo-activated by shining light of an appropriate wavelength on the system. After illumination, the attached molecules become charged via a photodissociation process or excited into a charge-separated state (thus generating a significant electric dipole). We carry out Brownian Dynamics simulations of ion flow through the channel in the presence of the additional charges generated in this fashion. Based on these calculations, we predict that photo-activation of appropriately positioned photo-sensitive compounds near the channel mouth can significantly modify the rate of ion permeation and the current rectification ratio. Possible implications for GlyR-based device designs are briefly discussed.

Keywords Engineering glycine receptor · Brownian dynamics · Computational modeling · Ion permeation · Photo-sensitive compound

M. H. Cheng · R. D. Coalson (✉)
Department of Chemistry, University of Pittsburgh, Pittsburgh, PA 15260, USA
e-mail: coalson@pitt.edu

M. Cascio
Department of Microbiology and Molecular Genetics, University of Pittsburgh School of Medicine, Pittsburgh, PA 15261, USA

M. Kurnikova
Department of Chemistry, Carnegie Mellon University, Pittsburgh, PA 15260, USA

Introduction

The glycine receptor (GlyR) and other members of the Cys-loop superfamily of ligand-gated ion channels (LGICs) are essential mediators of synaptic transmission in the central nervous system. These ionotropic receptors are pentameric membrane proteins. Each subunit of these receptors has a globular ligand-binding amino-terminal extracellular domain (ECD) and four transmembrane segments (TM1–TM4), with residues of TM2 lining the central gated pore, and a long, less well-conserved intracellular loop (connecting TM3 and TM4). In response to neurotransmitter binding to the ECD, the central pore transiently opens, allowing the passive movement of small ions down their electrochemical gradient across the lipid membrane in which the Cys-loop receptors are embedded (for reviews, see [1–3]). This ion flux changes the potential across the membrane, affecting the probability of opening of voltage-gated channels. Over the past few decades, ligand-gated ion channels, e.g., the nicotinic acetylcholine receptor (nAChR), have been successfully rendered responsive to light using synthetic photosensitive compounds [4, 5]. A ligand-gated channel engineered so as to incorporate a photoactivated switch may potentially be useful for converting an optical input into neuronal signaling or for providing a way to optically induce targeted drug delivery [6].

Research to date has focused primarily on the alteration of natural channel gates by synthetic photosensitive compounds [6, 7]. Here we address another potential design theme involving such engineered channels, namely, so as to enable the possibility for optical regulation of *ion permeation characteristics*. This general motif has been explored before in the context of Gramicidin A (GA) by Woolley and coworkers [8, 9]. These investigators engineered optically switchable dipolar molecules on the outside of the GA pore (i.e., in the lipid bilayer membrane region, next to the pore) in

such a way that when the external dipoles were switched on, the conductance of the pore was altered as a result of the change in the electrostatic forces on the permeant ions. Here we focus on the homopentameric human α1 GlyR to investigate whether similar effects may be produced in a suitably engineered LGIC. For reasons given below, the motif that we suggest involves attachment of photo-switchable moieties to the intracellular vestibule of GlyR—this accessible region of the channel is well-suited for chemical modification and attachment of additional sensing elements. Our choice of GlyR as the focus of the investigations reported here is further motivated by our previous experience modeling this channel—the success of the computational model that we have developed in previous applications [10–12] encourages us to think more broadly about the channel's natural properties, as well as novel properties that may be introduced by molecular level engineering.

In the present study, we utilize a Dynamic Monte Carlo (DMC) simulation technique [10, 13–16] to carry out Brownian Dynamics (BD) simulations in order to predict ion permeation characteristics in the photo-activated state of a photosensitive-GlyR channel. The photosensitive GlyR was configured by computationally incorporating point charges to represent the charged state of covalently bound photosensitive moieties at targeted sites in a model of the conduction pore that includes the five pore-lining M2 helices only, as described in Ref. [10]. In that earlier study, we successfully utilized DMC to calculate current through GlyR, including the large change in +/− ion selectivity observed in the mutant A251E GlyR. In the present study, this homopentameric GlyR model will be utilized to guide the optimal placement of photo-activated switch molecules in the vestibule of the GlyR. The outline of the paper is as follows. In the Methods section, we briefly review the DMC simulation technique, and specify the details of the model GlyR pore, including the attachment of photosensitive compounds to the vestibules leading into the pore. In the Results section, we present the results of our DMC simulations for two types of photosensitive species, namely (i) one that is photo-activated to a −1 charged molecular group, and (ii) one that is photo-activated into a zwitterionic form (a large induced dipole generated by polarization of electronic charge upon photoactivation). Finally, Discussion and Conclusions are supplied, including possible device design implications.

Methods

A Dynamic Monte Carlo technique

In DMC ion permeation simulations, the permeant ions are treated as spherical particles and the motion of ions is tracked explicitly, but the water and protein/membrane atoms are treated as continuous dielectric media. In our DMC algorithm for ion permeation [10, 13–16], configurations are generated by random changes of the ion positions. The total number of ions is characterized by $N = N_L + N_R + N_I + N_v$. Here N_L and N_R are the fixed numbers of ions (i.e. Na^+ and Cl^-) on the left and right boundaries (buffer regions in Fig. 1), which are obtained by integrating the given boundary concentrations C_L and C_R over the volumes of the boundary layers. In this study, the constant concentration boundary condition is imposed by randomly distributing N_L or N_R ions in the buffer regions at each Monte Carlo (MC) cycle [14]. N_I is the number of ions inside the system and N_v is the number of virtual ions. The total number of ions N is fixed and N_I fluctuates. N_v is introduced only for counting purposes and is included to account for dynamic fluctuation of the number of ions in the interior of the system, and to ensure the proportionality of Monte Carlo cycles to real time [13]. One Monte Carlo cycle consists of N steps. At each Monte Carlo step, one ion k is randomly chosen to move $\pm h_z$ in one direction (x, y, or z) if $Rand < \exp(-\beta\Delta W)$, where $Rand$ is a random number that lies in the interval [0, 1] and $\beta = (k_B T)^{-1}$. Furthermore, h_z is a position-dependent displacement (z being the position along the channel axis) determined by the diffusion constant profile. The diffusion constants and the associated ion displacements taken in one DMC step obey the relation:

$$h_z^2/D(z) = h_0^2/D_0 \tag{1}$$

where h_0 and h_z are the associated ion displacement in the bulk and at position z, respectively, and D_0 and $D(z)$ are the

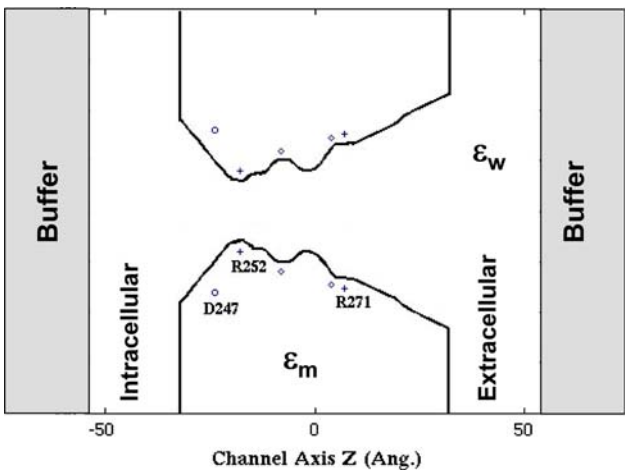

Fig. 1 Schematic depiction of the pore profile of the GlyR model. The protein channel and membrane extend from $z = -32$ Å to $z = 32$ Å, characterized by a uniform dielectric constant $\varepsilon_m = 5$. Effective charges and dipole moments are assigned to represent associated charges and dipoles on the pore lining TM2 segments. The dielectric constant in the water bath ε_w is taken to be the same as that inside the channel, namely, $\varepsilon_w = 80$ in all aqueous regions (including buffer regions). Gray regions represent buffer regions where a constant number of ions are maintained during DMC simulations

diffusion constants of ion in the bulk and at position z, respectively. ΔW is the energy change between the two configurations based on the chosen particle k with charge q_k [10]:

$$\Delta W = W_k^{new} - W_k^{old} \tag{2}$$

$$W_k = q_k\phi^{stat} - k_BT\ln(D(z)/D_0) + q_k^2\phi_k^{self} + \sum_{j\neq k}\frac{q_kq_j}{\varepsilon_w}\phi^{coul}(r_{kj}) + \sum_{j\neq k} q_kq_j\phi_{kj}^{diel} \tag{3}$$

where the first term in Eq. 3 is the electrostatic potential energy of ion k due to fixed charges on the pore forming protein/membrane, and any externally applied electric potential. In the present study, fixed charges on the pore forming protein channel include effective charges and dipole moments from the GlyR itself as well as those associated with the photo-activated versions of the inserted photo-sensitive compounds. ϕ^{stat} can be obtained by solving Poisson's Equation. The second term properly accounts for a position-dependent diffusivity profile within the context of a Brownian Dynamics simulation. (In particular, the gradient of the diffusivity profile contributes an additional term to the drift force that directs the motion of the Brownian particles, i.e., the permeant ions, in the solvent.) The third term accounts for the image potential due to the surface charge induced on dielectric boundaries by ion k. The fourth term describes Coulombic interactions between pairs of ions in an environment characterized by the (uniform) water dielectric constant ε_w, and the fifth term corresponds to the image potential experienced by ion k due to the surface charge induced by ion j. Calculation of the image potential and ion-ion interaction in a dielectrically inhomogeneous medium followed the same algorithm used in previous studies [10].

Construction of a model of the GlyR pore

The model GlyR pore itself is depicted in Fig. 1. A detailed description of the channel geometry, simulation parameters and the embedded fixed charges due to the protein channel can be found in Ref. [10]. Briefly, the cytoplasmic (intracellular) and extracellular regions are represented by funnel-like pores attached on either side of the transmembrane portion of the channel. The entire pentameric protein channel extends from $z = -32$ Å to $z = 32$ Å (cf. Fig. 1). Two dipole rings (diamonds), 5 dipoles per ring, were inserted (with the + end of the dipole pointing in towards the pore) in order to account for the electrostatic potential generated by the hydrophilic residue pairs (i) T259 and T258 at $z = -8$ Å, and (ii) T262 and G269 at $z = 4$ Å. Two rings of positive charge (5 charges per ring) were inserted to account for the arginine residues (plus signs) R252 and R271 located at $z = -18$ Å and $z = 7$ Å, respectively. A ring of 5 negative charges was inserted to account for aspartate D247 residues (circles) located at $z = -24$ Å. Values of the charges and dipole moments were selected to reflect various physical constraints suggested by the structural model (e.g., R252 resides in a very constricted section of the pore: hence the occupancy of water molecules near this section is limited, thus leading to an effective charge which is larger than that of R271, which resides in a water cavity [17, 18]. In the present study, these effective charges and dipole moments due to the GlyR itself were taken to be the same as in our previous study of ion permeation in this channel [10]. Specifically, the effective dipole moments of pore lining hydrophilic residues were assumed to be 0.3 D at both $z = -8$ Å and $z = 4$ Å, respectively. Furthermore, the effective charges of residues D247, R252 and R271 were chosen to be $-0.2e$, $0.3e$ and $0.2e$, respectively (e is the proton charge). The effective charges and dipole moments specified above were calibrated iteratively based on experimental current–voltage (I–V) curves obtained by Cascio et al. [19] and fine-tuned to reproduce an additional set of experimental results, i.e., the permeability ratio and I–V curve in a mutant A251E GlyR channel [20]. The dielectric constant in the water bath, ε_w, was taken to be the same as that inside the channel, namely, $\varepsilon_w = 80$ in all aqueous regions. A uniform dielectric constant of $\varepsilon_m = 5$ was assumed for the entire protein-membrane system, extending this region laterally outward from the protein pore (including the extracellular and cytoplasmic domains, which in this simple model are represented as extended membrane regions: cf. Fig. 1). The diffusion coefficient for both Na^+ and Cl^- was assumed to be $D = 2.0 \times 10^{-5}$ cm^2/s in the bulk, linearly reduced from this bulk value at the channel entrance ($z_L = -32$ Å and $z_R = 32$ Å) to half the bulk value at the transmembrane channel mouth ($z_L = -27$ Å and $z_R = 10$ Å), and maintained at half the bulk value throughout the transmembrane domain -27 Å $< z < 10$ Å [10].

The major goal of the present study is to investigate, computationally, the degree to which it may be possible to significantly modify the permeation of ions through GlyR in real time by subjecting a single channel molecule to an appropriate experimental perturbation, namely, illumination with light of a particular wavelength. For the Cys-loop superfamily, it is known that the net charge near the intracellular entrance plays a critical role in determining channel selectivity [1]. For the case of the wild type (WT) human α1 GlyR, mutation of (neutral) alanine to glutamate (negatively charged under physiological conditions), i.e., A251E, has been shown experimentally to render the channel cation selective (favor Na^+ flow over Cl^- permeation) [20, 21]. Indeed, the DMC simulations carried out in Ref. [10] were able to reproduce this effect. Consequently,

we have focused in the present study on using the photo-activated switch motif introduced by Kocer et al. [7] (in a different context) to mimic the A251E mutation as closely as possible. As shown by Kocer et al., photo-reaction of one of two types of molecular moiety attached to the pore lining can generate either one negatively charged monopole (where there was no charge before) or a +/− zwitterion (large dipole). Since the compounds involved are somewhat bulky, and the pore of the open GlyR channel is narrow (∼3 Å) [10, 11], we consider here a scenario where they are attached to the vestibule leading into the pore, which is much wider. Thus, the critical question arises as to what is the optimal position (and in the case of the zwitterions, orientation) at which to attach the photo-switchable molecules in order to achieve a large electrostatic effect; cf. Fig. 2. To investigate these issues, we have carried out extensive DMC simulations of channel conductance on the model GlyR system described above appropriately modified by attaching these two types of photo-sensitive compounds at different positions along the channel vestibule.

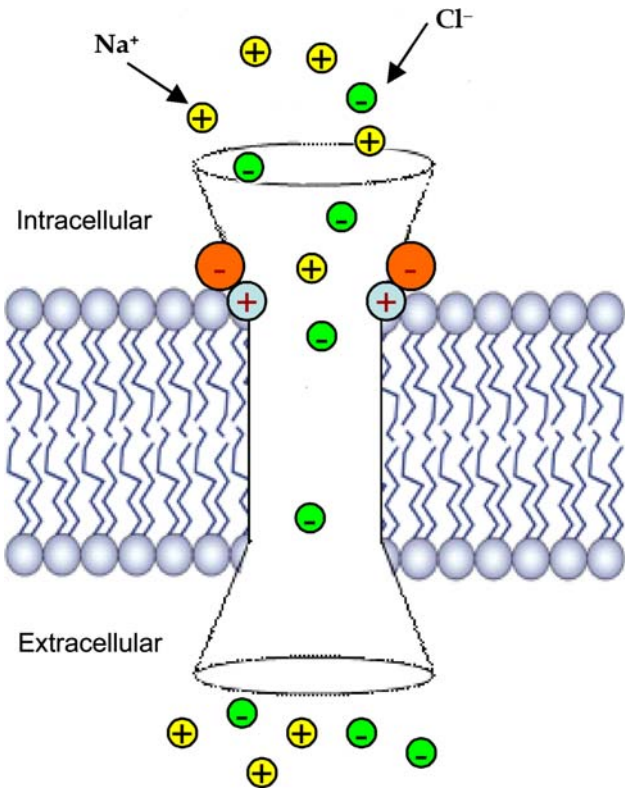

Fig. 2 Scheme for photo-activated switch control of ion permeation in GlyR. The selectivity filter (near positively-charged R252) in WT GlyR is represented by cyan circles with red plus sign in this highly schematic representation of the receptor in the lipid bilayer. Orange circles with minus sign represent the induced charges on the attached organic molecules

Results

Simulation results with photo-induced anionic groups (monopole effect)

Kocer et al. demonstrated that a molecule of the type shown in Fig. 3 can be attached to an arbitrary residue of the pore-lining portion of an ion channel [7]. Furthermore, photolysis at UV wavelengths (<300 nm) causes the indicated dissociation reaction, which leaves a −1 charged anionic moiety (essentially a carboxylate group) attached to the GlyR. The creation of additional negative charges inside the modified GlyR generates new electric fields that perturb the flow of ions through the channel. It is in principle possible that these charges can electrostatically hinder the entrance of anions and facilitate the entrance of cations, thus altering the ion selectivity of the channel. (N.B.: WT GlyR allows only anions to pass.) The effect on channel conductance depends strongly on the positions along the channel at which the switchable anionic moieties are attached. Two different sets of numerical simulations were performed in WT GlyRs modified by considering such attachments, assuming a symmetric 0.15 M NaCl bathing solution in both cases. In one set (cf. Fig. 2), five negatively charged groups (one for each subunit in the GlyR) were inserted near the intracellular mouth (6 Å toward the intracellular domain from positively charged R252 and 1 Å inside the channel); in a second set, the same set of anionic fragments were inserted near the extracellular mouth (6 Å toward the extracellular domain from positively charged R271 and 1 Å inside the channel). Keeping the pore radius and other charges and dipole moments the same as for the WT GlyR, the effective charge of this attached anionic fragment was assumed to be −0.2e in our simulations. It should be noted that the effective charges used in a continuum model are an approximate distillation of complicated microscopic phenomena. The optimal choice of these charges is affected, for example, by screening effects due to the neighboring amino acids or water, and the values of assigned dielectric constants. For this reason, in this study, the effective charge carried by this photo-sensitive molecule was taken to be the same as that of the D247 residue, which was assumed to carry an effective charge of −0.2 e, as in our previous calculations [10]. Furthermore, the photo-generated tethered anionic charge group was represented as a simple point charge, ignoring all other

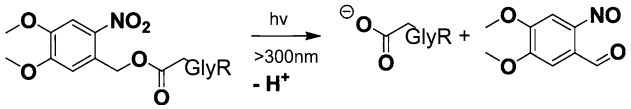

Fig. 3 Photolysis produces a tethered -1 charge (anionic) moiety at targeted sites on GlyR. [Adapted from Ref. [7]]

molecular details (e.g., perturbations in local structure). While perhaps overly simplistic (see Discussion and Conclusions section below), such treatment has proven successful in accounting for electrostatically induced perturbation of ion permeation due to mutations that modify the distribution of fixed charge lining the ion channel pore in BD simulations conducted on related systems [10, 22].

As expected, the current is reduced in both sets of simulations relative to the value obtained in the wild-type channel. However, the rectification ratio (cf. Fig. 4) is significantly different in the two cases. In the model channel where anionic groups are inserted near the extracellular mouth, there is no obvious current rectification and the computed current-voltage curve is found to be nearly linear, with currents about two times smaller in magnitude than for the WT channel. In contrast, when anionic fragments are inserted near the intracellular mouth, the channel is predicted to become outwardly rectifying with a rectification ratio $\gamma_{+60mv}/\gamma_{-60mv} = 3.2$, where $\gamma_{\pm 60mv}$ is the ionic current at an applied voltage of ± 60 mV, whereas in the wild-type GlyR the calculated rectification ratio is roughly $\gamma_{+60mv}/\gamma_{-60mv} = 1.0$ (i.e., it is non-rectifying). Note that in the case of anionic groups placed near the intracellular mouth (Fig. 4a), the Cl^- current is suppressed by nearly a factor of 10 at a modest applied voltage of -60 mV, thus suggesting that large changes in ion channel activity (specifically, ion permeation rates) can be effected by well-placed engineered charged groups located near the GlyR channel mouth, especially near the intracellular entrance.

The difference in rectification propensities observed when the ring of anionic charges is inserted into the intracellular versus the extracellular mouth can be traced to the asymmetry in the channel geometry: more specifically, the fact that the conical vestibule leading into the central channel pore is narrower on the intracellular side of the channel than the extracellular side. Thus a charge on the ring inserted in the intracellular vestibule is situated 6.0 Å from the channel centerline, while a charge on the ring inserted in the extracellular vestibule is 8.2 Å from the channel centerline. The electric field generated near the channel centerline is expected to be significantly stronger in the case of the intracellular vestibule ring insertion due to the increased proximity of the ring charges, and hence more effective in blocking the flow of Cl^- ions. Concerning the clearly discernable rectification signature observed in the case of negative charge ring insertion in the intracellular mouth of the channel, note that negative voltages applied in our simulations correspond to outward flow of Cl^-, and, conversely, positive voltages correspond to inward flow. When the photo-induced charges are located near the intracellular entrance, they are naturally more effective at blocking the entrance of Cl^- from the intracellular side than from the extracellular side at the same magnitude of applied voltage. As a result, a reduced Cl^- flow rate is obtained from the intracellular side.

Further computations (results not shown) reveal that both modified channels remain selective for chloride ions (over sodium ions). Increasing the total amount of negative charge carried by these anionic molecules (for example, putting 10 anionic fragments around the perimeter of the channel instead of 5) does not change the ion selectivity, but the channel modified near intracellular mouth becomes more strongly outwardly rectifying ($\gamma_{+60mv}/\gamma_{-60mv} = 5.0$).

Simulation result with photo-induced zwitterions (dipole effect)

Kocer et al. [7] have also demonstrated that a reversible photoswitch can convert the large mechanosensitive ion channel MscL into a valve that can be opened and closed, reversibly, by optical signals. In particular, irradiating this photosensitive molecule with 366 nm UV light results in a charged zwitterionic merocyanine (MC) structure while exposure to visible light (>460 nm) results in the original uncharged spiropyran (SP) state; cf. Fig. 5. A reversible photoswitch offers great potential for protein channel engineering applications, since it allows switching between different states rapidly and repeatedly [7]. To predict the

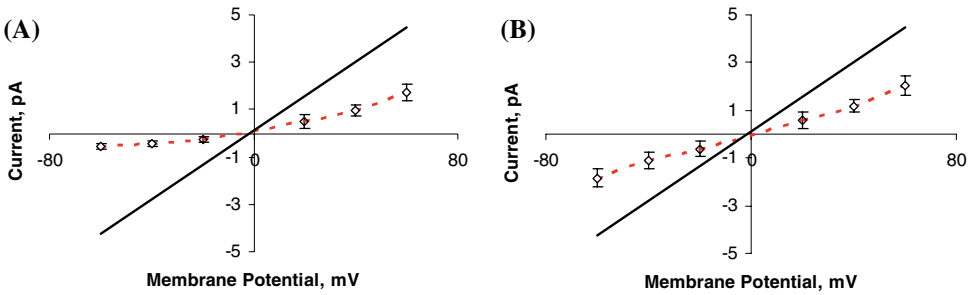

Fig. 4 Computed current-voltage curves obtained under symmetric 0.15 M NaCl bathing solution conditions in a modified GlyR channel (**a**) with five -0.2e anionic groups inserted near the intracellular mouth and (**b**) with five -0.2e anionic groups inserted near the extracellular mouth. Open diamonds with error bars (connected by red dashed lines) represent DMC simulation data in the modified channels. Solid black lines indicate linear fit of the results of DMC simulation of WT GlyR

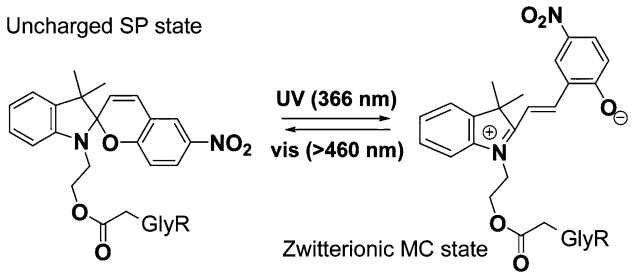

Fig. 5 Photolysis reversibly switches the tethered photo-sensitive molecule from the uncharged spiropyran (SP) state to a charged zwitterionic merocyanine (MC) state at targeted sites on GlyR. [Adapted from Ref. [7]]

possible effect of attaching these zwitterions to the GlyR, we performed DMC calculations in an appropriately modified GlyR. In this set of simulations, five zwitterionic molecules were inserted near the intracellular mouth (cf. Fig. 6a), in place of the five anionic fragments employed in the previous simulation. The negatively charged end was taken to face the channel lumen and the distance between "+" and "–"end was assumed to be 7.5 Å. The effective charges carried by the "–" and "+" end were assigned as −0.2e and 0.2e, respectively. Again, the zwitterionic molecule was represented simply by these additional two charges in the dipolar configuration just described: all other details of the attached molecule were ignored in our model system. The modified channel was found to be outwardly-rectifying with a rectification ratio $\gamma_{+60mv}/\gamma_{-60mv}$ = 2.2 (cf. Fig. 6b), slightly smaller than that in the model channel modified by attaching anionic fragments. Under an applied external potential of −60 mV, the current obtained was over two times smaller than that in the WT GlyR.

Note that even though these responses are less pronounced than in the case of the monopole switch described in the previous sub-section, they should be easily detectable. Their advantage over the monopole motif is that the zwitterionic dipoles can be switched on and off reversibly, thus making them much better candidates for device design, as discussed below.

Discussion and conclusions

The primary goal of this work has been to use modern computational techniques to suggest a design motif for modified biological ion channels whose function can be controlled at a single molecule level by application of an external stimulus, in this case light in a well-defined frequency range. The calculations presented herein are meant to be qualitative guides rather than quantitative predictions. In particular, we have shown via a computational approach that introduced point charges can control ion permeation characteristics in the GlyR (given that the introduced moieties are modeled as point charges, these calculations ignore any effects of the inserted compounds on channel structure). This suggests that attached photo-sensitive molecules near the channel entrance may significantly modify the ion permeation rates and the current rectification ratio of the channel, although according to our model calculations it is unlikely to change the channel selectivity.

We have chosen to explore the control paradigm presented above in the context of the GlyR, because in

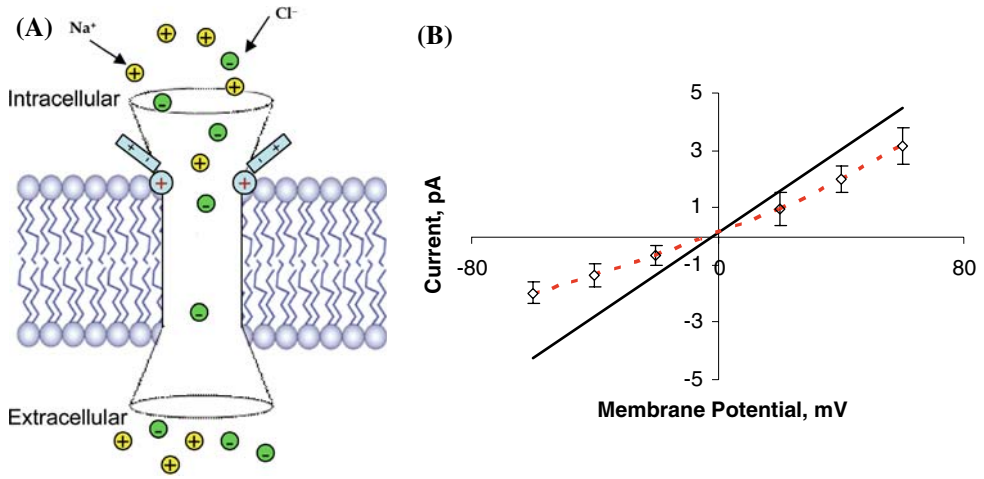

Fig. 6 (**a**) Scheme for photo-activated switch control of ion permeation in the GlyR. The selectivity filter (near positively charged R252) in WT GlyR is represented by cyan circles with red plus signs in this highly schematic representation of the receptor in the lipid bilayer. Sticks represent the induced dipoles in the attached organic photo-sensitive molecules (+/− ends are indicated). (**b**) Current-voltage curve obtained under symmetric 0.15 M NaCl bathing solution conditions in a wild-type GlyR channel modified with five zwitterionic (dipolar) photosensitive molecules inserted near the intracellular mouth. (Dipole characteristics are detailed in the text.) Open diamonds with error bars (connected by the red dashed lines) present DMC simulation data in the modified channels. The solid black line indicates a linear fit of DMC simulation results in the WT GlyR

previous work [10] we have painstakingly constructed a structural model of this pore (based on currently available NMR [23] and biochemical data, and by homology modeling to the full-length nAChR, as determined by cryo-electron microscopy [24]), and have carried out extensive current–voltage calculations using this pore model. These computations yielded current predictions that were in good agreement with extant experimental data. The only difference in the present system is the introduction of strategic vestibule-lining charges. Based on previous experience with Brownian Dynamics (and related Poisson–Nernst–Planck) studies of GlyR [10, 22] and other ion channels [25–29], it seems reasonable to expect that trends in the I–V curve behavior associated with the introduction of these charges should be predicted well by the BD model utilized here. The structural details of the attached chemical moieties were intentionally ignored in the exploratory calculations presented in this work. This aspect of the computation can be refined, for example, via Molecular Dynamics simulations to sample accessible configurations of the molecular groups attached to the vestibule lining [30]. Since we do not expect these additional details to change the qualitative conclusions of the present study, we leave them for further work (to be guided by planned experimental efforts to build engineered channels along the lines suggested in the present paper).

Finally, one possible device application of the motif developed here is as a chemical sensor whose output is tunable by light. For example, the simulations presented herein anticipate a glycine sensor wherein the permeation rate and current rectification ratio may be controlled by illumination with a particular wavelength (range) of light. Given the relatively large surface area and solvent accessibility of the channel vestibule, it should be feasible to incorporate single photo-switch molecules at multiple locations in each subunit via site-directed mutagenesis and subsequent chemical modification. The resulting receptor would act as a logical AND circuit, with the output dependent on the presence of glycine (the sensor component) AND light, with the degree of functional control of permeation being dependent on the positioning of the photo-switch—the extreme case being an on-off switch. (Note: this distinguishes the present motif with the GA motif demonstrated earlier by Woolley and coworkers [8, 9]. Their motif lacks the "second" input signal, namely gating of the channel by a chemical agonist, glycine.) We hypothesize that by utilizing other design modifications, where the ligand specificity and/or sensitivity of the receptor is significantly altered, for example by mutagenesis of the ligand binding site, could produce receptors that function as novel sensors. To illustrate one possible scenario, assume that a family of photo-activated switches can be made, each of which is activated by a different wavelength of light. Then, each of these switches could be attached to one of several mutant GlyR constructs with a wide range of EC_{50} values (such that the effective dose–response of the ensemble of constructs may be effectively calibrated over a wide concentration range). By illuminating the system with a wavelength of light that switches on one (and only one) channel construct at a time, ion conduction could be assigned to discrete subpopulations of the receptor. This puts a bound on the glycine concentration in the external bathing solution. By examining all the channels in this way, the concentration of glycine in the solution could be determined (within the dynamic range of the receptors' dose–response curves) from an output that is a function of both light and agonist concentration. Of course, this scenario is purely hypothetical at the moment. The first step would entail engineering the basic photo-switch motif suggested in this paper: device design issues would then become the focus of subsequent work.

Acknowledgements We wish to thank S. Essiz for her valuable assistance preparing the figures. We gratefully acknowledge computational support from Center for Molecular and Materials Simulation (CMMS) at the University of Pittsburgh. The work of MHC and RDC was supported in part by NSF Grant No.CHE-0518044 and ARO-MURI Grant No. DADD19-02-1-0227.

References

1. Lynch JW (2004) Physiol Rev 84:1051
2. Cascio M (2004) J Biol Chem 279:19383
3. Keramidas A, Moorhouse AJ, Peter PR, Barry PH (2004) Prog Biophys & Mol Biol 86:161
4. Bartels E, Wasserman NH, Erlanger BF (1971) PNAS 68:1820
5. Lester HA, Krouse ME, Nass MM, Wassermann NH, Erlanger BF (1980) J Gen Physiol 75:207
6. Banghart MR, Volgraf M, Trauner D (2006) Biochemistry 45:15129
7. Kocer A, Walko M, Meijberg W, Feringa B (2005) Science 309:755
8. Borisenko V, Burns DC, Zhang Z, Woolley GA (2000) J Am Chem Soc 122:6364
9. Lougheed T, Borisenko V, Hennig T, Rueck-Braun K, Woolley GA (2004) Org Biomol Chem 2:2798
10. Cheng MH, Cascio M, Coalson RD (2005) Biophys J 89:1669
11. Cheng MH, Cascio M, Coalson RD (2007) Proteins 68:581
12. Cheng MH, Coalson RD, Cascio M (2008) Proteins 71:972
13. Graf P, Nitzan A, Kurnikova MG, Coalson RD (2000) J Phys Chem B 104:12324
14. Cheng MH, Mamonov AB, Dukes JW, Coalson RD (2007) J Phys Chem B 111:5956
15. Cheng MH, Coalson RD (2005) J Phys Chem B 109(1):488
16. Graf P, Kurnikova MG, Coalson RD, Nitzan A (2004) J Phys Chem B 108:2006
17. Lobo IA, Mascia MP, Trudell JR, Harris RA (2004) J Biol Chem 279:33919
18. Lynch JW, Han NL, Haddrill J, Pierce KD, Schofield PR (2001) J Neurosci 21:2589
19. Cascio M, Shenkel S, Grodzicki RL, Sigworth FJ, Fox RO (2001) J Biol Chem 276:20981
20. Keramidas A, Moorhouse AJ, Pierce KD, Schofield PR, Barry PH (2002) J Gen Physiol 119:393

21. Moorhouse AJ, Keramidas A, Zaykin A, Schofield PR, Barry PH (2002) J Gen Physiol 119:411
22. O'Mara M, Barry PH, Chung SH (2003) PNAS 100:4310
23. Yushmanov VE, Mandal PK, Liu Z, Tang P, Xu Y (2003) Biochemistry 42:3989
24. Unwin N (2005) J Mol Biol 346:967
25. Kurnikova MG, Coalson RD, Graf P, Nitzan A (1999) Biophys J 76:642
26. Im W, Roux B (2002) J Mol Biol 322:851
27. Corry B, O'Mara M, Chung S-H (2004) Biophys J 86:846
28. Cardenas AE, Coalson RD, Kurnikova MG (2000) Biophys J 79:80
29. Coalson RD, Kurnikova MG (2005) IEEE Trans Nanobiol 88:3745
30. Jun S, Becker JS, Yonkunas M, Coalson RD, Saxena S (2006) Biochemistry 45:11666